Structure and Dynamics of Barnase Complexed with 3′-GMP Studied by NMR Spectroscopy†

Elizabeth M. Meiering,‡ Mark Bycroft, Michael J. Lubienski, and Alan R. Fersht*

MRC Unit for Protein Function and Design, Cambridge IRC for Protein Engineering, University Chemical Laboratory, Lensfield Road, Cambridge CB2 1EW, U.K.

Received April 29, 1993; Revised Manuscript Received August 2, 1993®

ABSTRACT: The binding of 3′-GMP to the ribonuclease, barnase, has been studied using heteronuclear 2D and 3D NMR spectroscopy. The ^1H and ^{15}N NMR spectra of barnase complexed with 3′-GMP have been assigned. 2D and 3D NOESY spectra have been used to identify inter- and intramolecular NOEs, and a solution structure for the barnase–3′-GMP complex has been calculated. The position of the guanine ring of the ligand is reasonably well defined in the structures. The guanine ring forms hydrogen bonds with the NH protons of Ser57 and Arg59. These residues are located in a loop that is conserved among the microbial guanine-specific ribonucleases. The 2′-hydroxyl of 3′-GMP is close to His102 and Glu73, which have been shown to be involved in catalysis. The phosphate group of 3′-GMP is close to a number of positively charged residues that have also been shown to be important for activity. The position of the sugar moiety of 3′-GMP is less well defined in the structures. Structures calculated for the complex could not simultaneously satisfy all the observed intermolecular NOEs for the sugar protons, suggesting that the sugar samples several conformations when bound to barnase. The binding of 3′-GMP to barnase in solution is similar to that observed in the crystal structures of nucleotides bound to related ribonucleases. 3′-GMP binding causes no major conformational change in barnase. In contrast to the small structural changes that occur, there is a significant decrease in the rates of hydrogen/deuterium exchange and aromatic ring rotation in the active site of barnase upon ligand binding.

Barnase is a small extracellular ribonuclease from *Bacillus amyloliquefaciens* (Hartley, 1989). It is a member of a family of microbial ribonucleases (Hartley, 1980; Hill et al., 1983) whose catalytic properties have been studied in detail by kinetics, chemical modification, site-directed mutagenesis, crystallography, and NMR spectroscopy [reviewed by Uchida and Egami (1971), Takahashi and Moore (1982), and Saenger (1991)]. The microbial enzymes catalyze the hydrolysis of RNA in two steps, similar to catalysis by bovine pancreatic ribonuclease A, although there is no sequence or structural homology between the microbial and mammalian enzymes. The first step is transphosphorylation to form a 2′,3′-cyclic phosphate intermediate, followed by hydrolysis of the intermediate to yield a fragment of RNA ending in a 3′-monophosphate. Two conserved residues, His102 and Glu73 in barnase, act as general acid–base groups during catalysis (Mossakowska et al., 1989; Steyaert et al., 1990). A conserved arginine, Arg87 in barnase, is also important for activity. It helps form the structure of the active site and may interact with the reactive phosphate group (Meiering et al., 1991). The enzymes cleave RNA at guanine nucleotides. A conserved loop, consisting of residues **Phe56**-Ser57-**Asn58**-Arg59-**Glu60**-Gly61 in barnase (conserved residues are in bold type), is involved in binding the guanine base (Sevcik et al., 1990).

The best characterized enzymes in the family are barnase and RNase T1, the ribonuclease from *Aspergillus oryzae* (Heinemann & Hahn, 1989; Pace et al., 1991). These two enzymes have only 20% sequence identity, and their activities are significantly different. Barnase is twice as active toward RNA as RNase T1, but RNase T1 is 1000-fold more active than barnase on dinucleotide substrates (Mossakowska et al., 1989). The enzymes also have different subsites for RNA (Osterman & Walz, 1978, 1979; Day et al., 1992, and references therein). Site-directed mutagenesis has revealed that several residues, not conserved between the two enzymes, are important for catalysis. These include Lys27 in barnase and His40 and Tyr38 in RNase T1 (Mossakowska et al., 1989; Steyaert et al., 1990).

Structural information is required in order to understand the molecular basis for the differences in activity. There is considerable structural information from X-ray crystallography on the recognition of RNA by the microbial ribonucleases (Sevcik et al., 1990), particularly RNase T1 [reviewed by Heinemann and Hahn (1989)]. However, there is relatively little information on barnase. The structure of free barnase has been determined by X-ray crystallography (Mauguen et al., 1982) and NMR (Bycroft et al., 1991), and the structure of barnase complexed with d(GpC) has been solved by X-ray crystallography (Baudet & Janin, 1991). In the complex, however, the primary recognition site is empty and the dinucleotide is bound outside the active site at the interface between two protein molecules, with the guanine interacting with a putative N_{+1} subsite. Here, NMR is used to study the binding of 3′-GMP to barnase in solution. The ^1H and ^{15}N spectra of barnase complexed with 3′-GMP are assigned, and the structure of the complex is determined from NMR data. Dynamic information is obtained from measurements of

† This research was supported by the Medical Research Council of the UK. E.M.M. was supported by the Natural Sciences and Engineering Research Council of Canada.

* Author to whom correspondence should be addressed.

‡ Present address: Department of Biological Chemistry and Molecular Pharmacology, Harvard Medical School, 240 Longwood Avenue, Boston, MA 02115.

® Abstract published in *Advance ACS Abstracts,* October 1, 1993.

0006-2960/93/0432-10975$04.00/0

hydrogen/deuterium exchange of the free enzyme and the complex.

MATERIALS AND METHODS

Protein Expression and Purification. Unlabeled wild-type barnase was purified from cultures of *Escherichia coli* containing the plasmid pMT410 (Hartley, 1988) as described previously (Mossakowska et al., 1989). Protein uniformly labeled with ^{15}N was prepared in the same way except that the casein amino acid hydrolysate was omitted from the medium and the ammonium chloride was replaced with [^{15}N]-ammonium chloride (98 atom %, Aldrich). Purified protein was dialyzed extensively against H_2O and then flash frozen and stored at −70 °C or lyophilized and stored at −20 °C.

UV Difference Spectroscopy. The dissociation constant for 3′-GMP and barnase was measured using UV difference spectroscopy. The UV difference spectrum of the barnase–3′-GMP complex relative to free barnase and 3′-GMP has a maximum at 290 nm and a minimum at 243 nm, similar to that observed previously for RNase T1 (Walz & Hooverman, 1973). The difference in absorbance at 290 and 243 nm ($\Delta\Delta A = \Delta A_{290} - \Delta A_{243}$) was measured upon titrating a solution of barnase (20 μM protein, 59.8 mM acetic acid/40.2 mM sodium acetate, pH 4.5) with a concentrated solution of 3′-GMP [disodium salt (Sigma) in H_2O]. The concentrations of the enzyme and ligand solutions were determined spectophotometrically using $A_{280_{0.1\%}} = 2.21$ cm^{-1} (Loewenthal et al., 1991) and $A_{253} = 13.7$ mM^{-1} cm^{-1} (Dawson et al., 1986), respectively.

NMR Spectroscopy. Samples for NMR spectroscopy were prepared by dissolving lyophilized protein in 90% H_2O/10% D_2O or 100% D_2O, briefly centrifuging the solution, and then measuring the protein concentration spectophotometrically, as above. An aliquot of a stock 3′-GMP solution (40–80 mM in H_2O or D_2O) was added to the protein solution to give a 1:1 barnase to ligand ratio. The pH or pD was then adjusted to 4.5 (uncorrected for isotope effect).

Spectra were acquired on a Bruker AMX 500 spectrometer equipped with either a 5 mm inverse probe or a triple-resonance $^1H/^{15}N/^{13}C$ probe. Proton chemical shifts were referenced to internal TSP at 0.07 ppm to correspond to the original assignments for wild-type barnase (Bycroft et al., 1990), and nitrogen chemical shifts were referenced to external $(^{15}NH_4)_2SO_4$ at 24.93 ppm. 2D spectra were processed using the Bruker program, UXNMR, on an X32 data station. The 3D NOESY-HMQC spectra were processed using the program FELIX (Hare Research, Inc.) on a Silicon Graphics 4D/35 Personal Iris.

In all experiments, solvent suppression was achieved by presaturation of the solvent signal during the relaxation delay, which was 1.5 s, and TPPI (Marion & Wüthrich, 1983) was used for sign discrimination in f_1. 2D ^1H spectra (DQF-COSY, TOCSY, and NOESY) of unlabeled barnase complexed with 3′-GMP were acquired and processed essentially as described by Bycroft et al. (1990). In addition, ^1H–^{15}N heteronuclear experiments were carried out on the labeled complex. In all these experiments, ^{15}N decoupling during acquisition was achieved using the GARP sequence (Shaka et al., 1985). Two-dimensional ^1H–^{15}N ^1H-detected single-quantum heteronuclear chemical shift correlation (HSQC) spectra (Bodenhausen & Ruben, 1980) were acquired using nonrefocused, INEPT magnetization transfers (Morris & Freeman, 1979) to minimize line widths and maximize spectral resolution (Bax et al., 1990). In order to identify NH groups of both the protein main chain and side chains, the ^{15}N spectral width was set to 6332 Hz and 512 t_1 increments were collected. The spectral width was 4000 Hz in the proton dimension, and 1024 complex data points were acquired. The transmitter frequency was switched from the water resonance to the middle of the NH region immediately prior to acquisition and switched back again immediately after. Data were zero-filled to give a 2048 (f_2) × 1024 (f_1) real matrix. A $\pi/2$ shifted sine bell was applied in f_2, and a weak Lorentzian–Gaussian apodization was applied in f_1 prior to Fourier transformation.

2D HMQC-NOESY and 2D HMQC-TOCSY spectra were acquired as described by Gronenborn et al. (1989) except that the TOCSY spectra were recorded using a DIPSI spin lock sequence (Shaka et al., 1988). The mixing times were usually 150 and 56 ms for the NOESY and TOCSY, respectively. In both experiments, 256 t_1 increments were collected over a spectral width of 3675 Hz, and 2048 complex data points were acquired in f_2 over a spectral width of 8064 Hz. The data were processed using shifted sine bells in both dimensions.

3D NOESY-HMQC spectra were recorded essentially as described by Marion et al. (1989). TPPI was used in f_1 and f_2. ^{15}N decoupling in f_1 was achieved using GARP (Shaka et al., 1985). The mixing time was 150 ms. In the f_1 ^1H dimension, 256 increments were acquired over a spectral width of 6400 Hz. In the f_2 ^{15}N dimension, 64 increments were acquired over 2500 Hz. A total of 512 complex data points were collected in the f_3 ^1H dimension over 4400 Hz, with O1 set to the middle of the NH region. The transmitter frequency was switched from the water resonance to the middle of the NH region immediately prior to acquisition and switched back again immediately after. Eight scans were acquired for each increment. The total time for the experiment was approximately 48 h. Data were zero-filled to yield a final matrix of 1024 (f_3) × 256 (f_2) × 512 (f_1) real data points. Mild Lorentzian–Gaussian apodization was applied in f_3, and sine bells shifted by $\pi/3$ were applied in f_1 and f_2 prior to Fourier transformation.

Hydrogen/Deuterium Exchange Rate Measurements. The exchange rates of protein NH protons with solvent deuterons was measured by following the decrease with time of the intensity of ^{15}N–^1H cross peaks of HSQC spectra of barnase and the barnase–3′-GMP complex dissolved in D_2O, at 26 °C. A protein sample in 100% H_2O, pH 4.5, was prepared as before. This sample was lyophilized and redissolved in D_2O to initiate exchange. The pD of the solution was quickly adjusted to 4.5. The solution was briefly centrifuged to remove small particles of undissolved material and put in an NMR tube. Acquisition of the first spectrum began 24 min after the sample was dissolved in D_2O. Initially, spectra were acquired one immediately after the other. Time gaps between spectra were introduced and gradually increased in length as the exchange proceeded. The last time point was taken after 114 days.

HSQC spectra were acquired as before except that, in order to decrease the acquisition time, the phase cycling was reduced to 4 steps (Marion et al., 1989) and 200 increments were used in f_1 which had a spectral width of 3675 Hz. Using these conditions, the time to acquire one spectrum was 18 min 37 s. The spectra were processed as before except that the data were zero-filled to 512 complex data points in f_1. The intensity of individual cross peaks was measured by volume integration using UXNMR. The decrease in cross peak volume with time was fit to the equation for a single-exponential decay plus an offset using nonlinear regression analysis with the program Kaleidagraph (Abelbeck, USA).

Resonance Assignments. The ^1H (Bycroft et al., 1990) and ^{15}N (Jones et al., 1993) assignments for free barnase were used as starting points for obtaining assignments for the complex. First the $C^\alpha H$–NH fingerprint region of the COSY spectrum of the complex was compared with that of free wild type. Peaks at the same positions were initially assumed to originate from corresponding protons in the two proteins. These assignments were confirmed and extended to residues in which protons have different chemical shifts from wild type using standard sequential assignment methods (Wüthrich, 1986) and comparisons with spectra of wild type. In the course of assigning the protein resonances, the resonances for 3′-GMP were also identified (see Results). Similarly, ^{15}N assignments of the protein in the barnase–3′-GMP complex were obtained by initially assigning peaks that occur at the same position in the HSQC spectra of the complex and free wild type to the equivalent nuclei in the two species. These assignments were confirmed and extended by checking for consistency with the ^1H assignments and identifying connectivities in the 2D HMQC-TOCSY, 2D HMQC-NOESY, and 3D HMQC-NOESY spectra. In the process of assigning the ^{15}N resonances, some additional assignments for some side chain protons were obtained.

Solution Structure Determination: Experimental Restraints. The structure of wild-type barnase in solution has been calculated previously from NMR data (Bycroft et al., 1991). The recording of 3D HMQC-NOESY spectra allowed the assignment of more NOEs than was previously possible using 2D ^1H NOESY spectra (Bycroft et al., 1991). These NOEs were converted into distance restraints as before. The ϕ and χ_1 angle restraints for the protein main chain and side chain, respectively, and intramolecular hydrogen-bond restraints for the protein were obtained as before (Bycroft et al., 1991).

The NOE spectra of the barnase–3′-GMP complex were analyzed in detail using the NOEs of free barnase as a reference. Spin diffusion can cause inaccuracies in determining distance restraints using NOEs for sugar protons. The effects of spin diffusion on the NOEs for the ribose ring protons of 3′-GMP were investigated by comparing spectra obtained with mixing times of 30, 60, 100, 150, and 220 ms. The NOE between H1′ and H2′ was used as a reference for a "medium" NOE since the distance between these protons is relatively insensitive to sugar conformation (2.8 ± 0.1 Å) (Wüthrich, 1986). There is little change in the relative intensities of the NOEs up to a mixing time of 150 ms, indicating that the effects of spin diffusion are small. The NOEs for the complex were, therefore, converted into distance restraints using a 150-ms NOESY spectrum in the same way as for free barnase. Angle restraints and hydrogen-bonding restraints for the protein were also obtained as before. Intermolecular hydrogen bond restraints between 3′-GMP and barnase were identified by the downfield shifts of ^1H and ^{15}N resonances in conjunction with NOE information and amide hydrogen exchange data (see Results).

Protocol for Structure Calculation. The structure for free barnase was previously calculated (Bycroft et al., 1991) using a two-stage distance geometry/simulated annealing procedure (Nilges et al., 1988) using the program XPLOR (Brünger, 1988) which is based on the molecular dynamics program CHARMM (Brooks et al., 1983). Here, structures of both free barnase and barnase complexed with 3′-GMP were calculated using simulated annealing from random coil starting structures (Brünger, 1988).

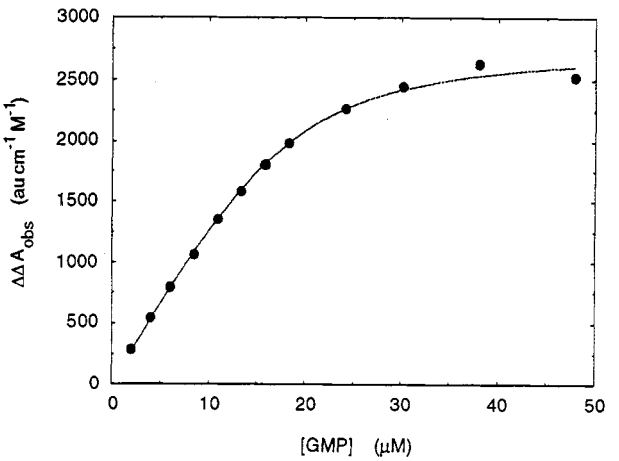

FIGURE 1: Plot of change in absorbance, $\Delta\Delta A_{obs}$, normalized with respect to enzyme concentration, as a function of 3′-GMP concentration for wild-type barnase at pH 4.5, 30.0 °C.

Initial structures of barnase were generated with random backbone configurations and extended side chains. These structures were used as input for dynamical simulated annealing calculations (Brünger, 1988). An initial 50 steps of conjugate-gradient (Powell mechanics) minimization, to ensure planarity of planar groups including hydrogens, were followed by 20 ps of restrained molecular dynamics at 1000 K, using a time step of 2 fs. Following the 20 ps of dynamics, the distance restraint potential and the van der Waals repulsive term were increased over 9 ps. Next, the temperature of the system was reduced, in steps of 25 K, to 300 K. This was followed by 200 steps of conjugate gradient minimization, to yield the "first-stage" structure. The "first-stage" structures were then refined in the second stage of the structure calculation using the simulated annealing protocol of Nilges et al. (1988).

The structure calculations for the complex were carried out in a similar way. Coordinates for 3′-GMP were derived from the coordinates of 3′-GMP in the crystal structure of the binase–3′-GMP complex (coordinates courtesy of Drs A. G. Pavlovsky and M. Ya. Karpeisky) by adding hydrogens and changing the glycosidic torsion angle, χ, to one of 10 different values ($\chi = 0 + 36j$; $j = 0$–9) using the program Insight II (Biosym Technologies, Inc.). The coordinates for 3′-GMP were placed at a random position relative to the random coil protein coordinates, and the combined coordinates used as input for the first dynamical simulated annealing calculation. In this stage, all the experimental distance and angle restraints for the protein and only the intermolecular distance restraints for H8 of 3′-GMP were used. This was necessary in order to maintain the chirality of the nucleotide (see Results). In the second stage, all the experimental restraints for both the protein and 3′-GMP were included.

In the calculations, standard values of the force field parameters for proteins and nucleic acids were used for barnase and 3′-GMP, respectively (Brünger, 1988). The calculations were carried out on an Alliant Concentrix 2800 2.2.00 computer. Structures were visualized on a Silicon Graphics 4D/35 Personal Iris using the program Insight II (Biosym Technologies, Inc.).

RESULTS

Measurement of Dissociation Constant for 3′-GMP. The binding of 3′-GMP by wild-type barnase was quantitated by measuring the difference absorbance changes upon titrating a solution of barnase with 3′-GMP (Figure 1). The data were

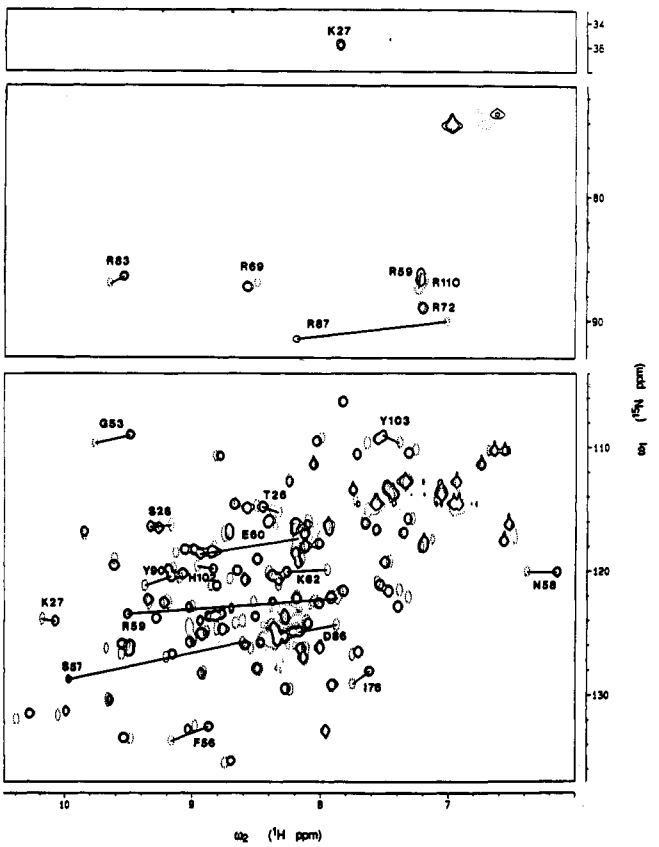

FIGURE 2: Overlay of ^1H–^{15}N HSQC spectra of uniformly ^{15}N-labeled barnase complexed with 3′-GMP (solid cross peaks) and free barnase (dotted cross peaks). Spectra were obtained in 90% H_2O/10% D_2O, pH 4.5, 37 °C. Cross peaks that are at different positions in the overlayed spectra are joined by lines and labeled by single letter amino acid code and residue number.

fit to the following single binding site equation using the program Kaleidagraph (Abelbeck, USA):

$$\Delta\Delta A_{obs} = \frac{\Delta\Delta A_{max}}{2}([E]_0 + [L]_0 + K_d - \sqrt{([E]_0 + [L]_0 + K_d)^2 - 4[E]_0[L]_0})$$

where $\Delta\Delta A_{obs}$ is the observed change in absorbance ($\Delta A_{290} - \Delta A_{243}$), $\Delta\Delta A_{max}$ is the maximum change in absorbance, $[E]_0$ is the total enzyme concentration, $[L]_0$ is the total ligand concentration, and K_d is the enzyme–ligand dissociation constant. A K_d value of 2.3 ± 0.3 μM was obtained.

Solution Structure Determination for Free Barnase. Analysis of the 3D NOESY-HMQC spectra of barnase revealed significantly more NOEs than could be resolved in the 2D ^1H NOESY spectra (Bycroft et al., 1991). The number of medium range [$(i-j) \leq 5$] NOEs was increased from 271 to 373 and the long range [$(i-j) \geq 5$] NOEs from 288 to 344. The new structures calculated with these constraints are significantly better defined than those reported previously (Bycroft et al., 1991). The backbone RMS deviation from the average structure is 0.69 Å compared with 1.22 Å in the previous study, while for all atoms the RMS deviation is 1.37 Å compared with 1.75 Å. The lower RMS values are the result of an improvement in the structure throughout the protein and are not confined to any particular region.

Analysis of NMR Spectra of the Barnase-3′-GMP Complex: Assignment of Protein Resonances. The spectra of the barnase–3′-GMP complex are similar to the spectra of free barnase (illustrated in Figure 2). Consequently, assignments for most of the ^1H and ^{15}N resonances in the complex could be obtained by comparison with the spectra of free wild type. Sequential assignment methods were required to obtain assignments for the guanine binding loop and for some other residues in the active site. The assignment of some side chain resonances is described in more detail below.

The $C^\delta H$ and $C^\epsilon H$ resonances of Phe56 in the complex are exchange broadened in spectra recorded between 5 and 49 °C, indicating that these protons are in intermediate exchange. The ring of Phe56 is in fast rotation in free barnase. This rotation is hindered in the complex by the packing of the guanine ring onto Phe56 (see Figure 8 and Discussion).

The heteronuclear spectra proved to be very useful for assigning side chain resonances. A substantial number of these are difficult or impossible to assign using only 2D ^1H spectra because of prohibitive spectral overlap. In particular, it was possible to obtain assigments for side chain ^1H and $^{15}N^\epsilon$ resonances for all six arginine side chains. This was done by identifying cross peaks between $^{15}N^\epsilon$ and $N^\epsilon H$, $C^\delta H$, $C^\gamma H$, $C^\beta H$, and, in some cases, $C^\alpha H$ in the 2D HMQC-TOCSY spectra (Figure 3) and correlating these with 2D ^1H COSY cross peaks. A new weak cross peak was identified in the HSQC spectrum of the complex at an ^{15}N chemical shift of 35.8 ppm and a ^1H shift of 7.84 ppm (Figure 2). This ^{15}N shift is characteristic of $^{15}N^\zeta$ resonances of lysine side chains. A new cross peak is also observed between a resonance at 7.84 ppm and a resonance at 3.13 ppm in the 2D ^1H COSY

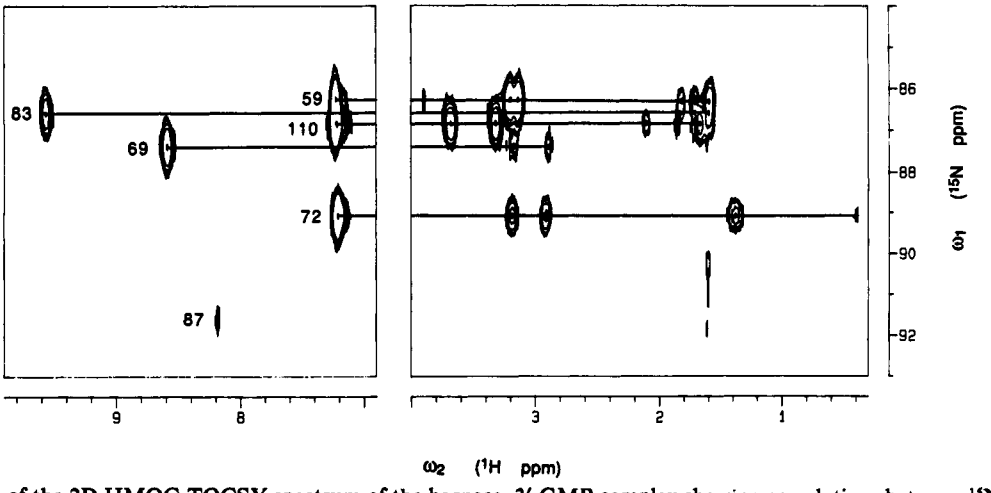

FIGURE 3: Section of the 2D HMQC-TOCSY spectrum of the barnase–3′-GMP complex showing correlations between $^{15}N^\epsilon$ and $N^\epsilon H$, $C^\delta H$, $C^\gamma H$, $C^\beta H$, and $C^\alpha H$ resonances of arginine side chains. Resonances from one side chain are joined by a horizontal line and labeled by residue number. The protein and 3′-GMP concentrations were approximately 5 mM, at pH 4.5, 37 °C.

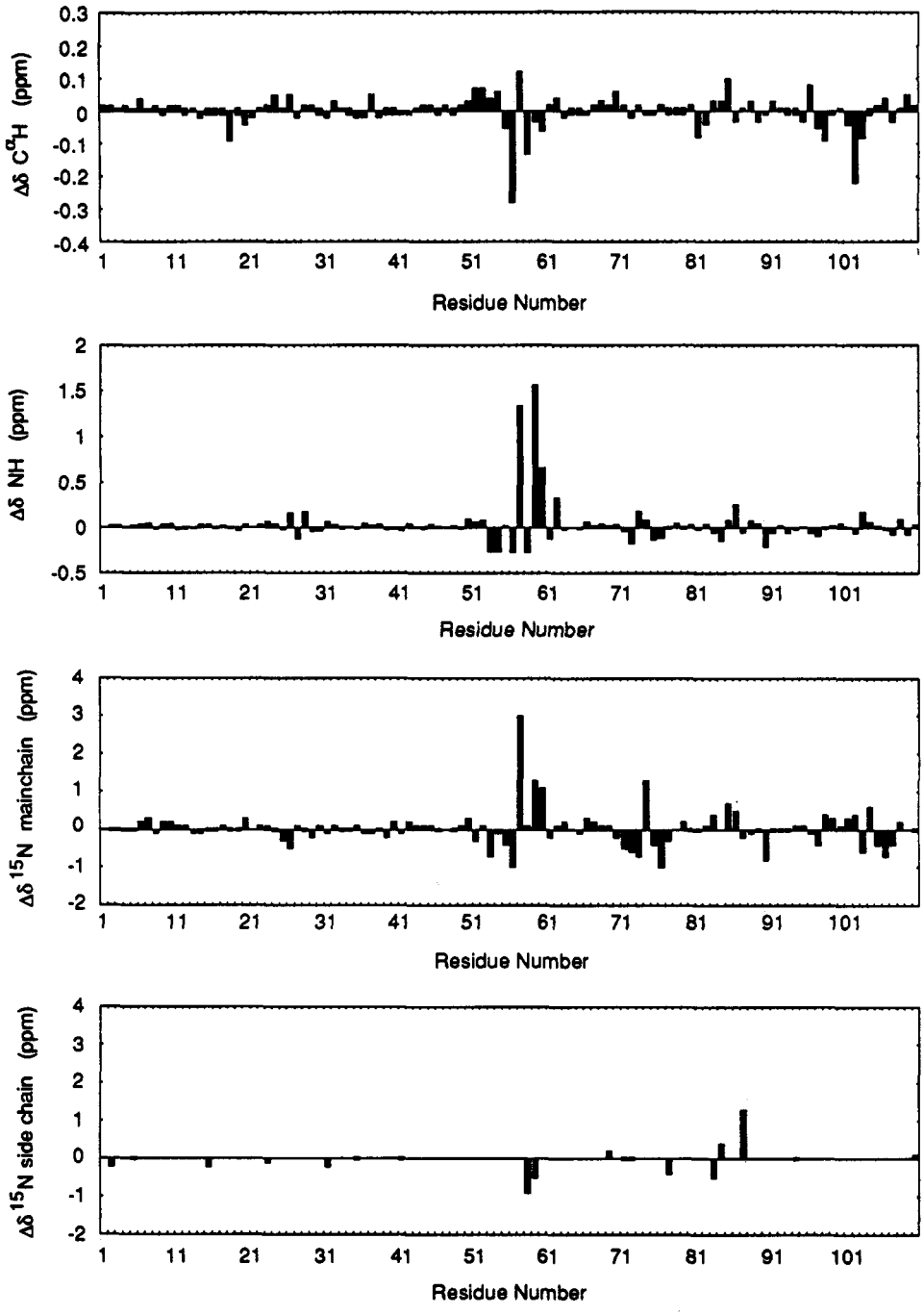

FIGURE 4: Chemical shift changes, Δδ, of main chain $C^{\alpha}H$, NH, and ^{15}N, and side chain ^{15}N resonances for barnase complexed with 3′-GMP relative to free barnase. Δδ is calculated by subtracting the chemical shift of resonances in free barnase from that in complexed barnase.

spectrum. These resonances have been tentatively assigned to the $N^{\zeta}H_3$ and $C^{\delta}H_2$ protons of Lys27, respectively. No other connectivities between these resonances and the rest of the side chain of Lys27 could be identified in ^1H–^{15}N spectra; however, there is a COSY cross peak at 3.13 ppm and 1.90 ppm which could be the $C^{\delta}H_2$–$C^{\gamma}H_2$ correlation. Although the data linking the $N^{\zeta}H_3$ and $C^{\delta}H_2$ resonances with the rest of the side chain are weak, the assignments seem reasonable for the following reasons: other resonances in the side chain of Lys27 and in the vicinity of Lys27 (e.g., in Asp54) are perturbed upon binding of 3′-GMP; the $N^{\zeta}H_3$ group of Lys27 is near the phosphate group of 3′-GMP in the NMR structure of barnase complexed with 3′-GMP (see Figure 9 and Discussion); Lys27 is involved in the binding of phosphate in the active site of barnase (Meiering et al., 1991). No cross peaks for $N^{\zeta}H_3$ of Lys side chains are observed in the HSQC spectrum of wild-type barnase, probably because in the free enzyme these protons are in fast exchange with H_2O. In the barnase–3′-GMP complex, the protons may become hindered to exchange, and hence NMR observable, due to an electrostatic interaction of the $N^{\zeta}H_3$ of Lys27 with the phosphate group of 3′-GMP.

The changes in chemical shift caused by 3′-GMP binding are shown graphically for the main chain NH, $C^{\alpha}H$, and ^{15}N resonances, and side chain ^{15}N resonances in Figure 4. The majority of the ^1H and ^{15}N resonances of barnase have similar chemical shifts in the complex and the free enzyme. Many nuclei in the active site, however, exhibit significant changes in chemical shift upon 3′-GMP binding. The largest changes occur for main chain and side chain nuclei of residues that have been implicated in guanine binding or catalysis. These include Phe56-Ser57-Asn58-Arg59-Glu60 (in the guanine binding loop), Glu73 and His102 (the general acid–base catalytic groups), Lys27 (another catalytic residue), and Arg87

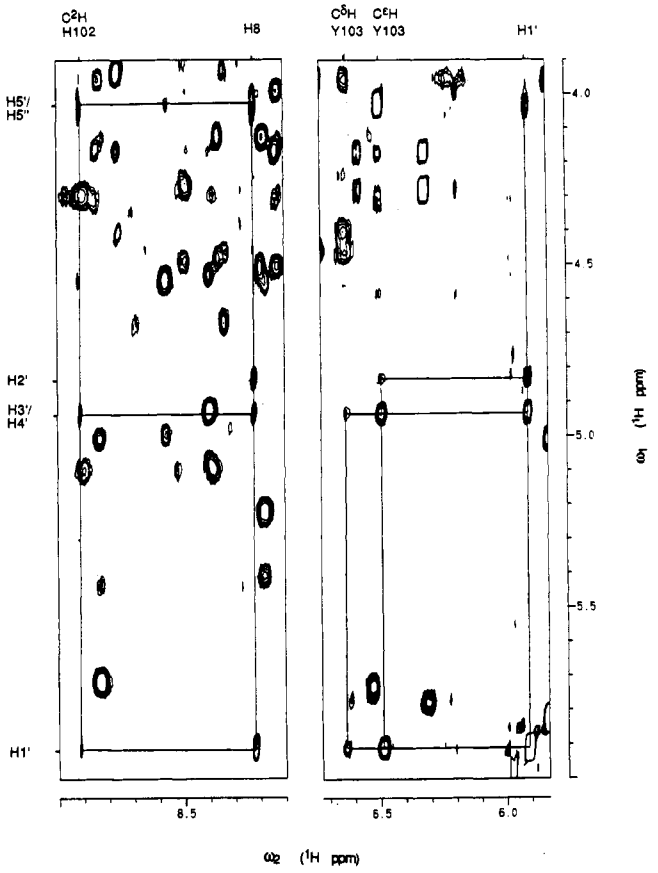

FIGURE 5: Section of NOESY spectrum of barnase–3′-GMP complex, at pH 4.5, 37 °C, showing intramolecular NOEs between H1′, H2′, H3′/H4′, H5′/H5″, and H8 of 3′-GMP, and intermolecular NOEs between 3′-GMP resonances and the C²H of His102 and C⁵H and C⁶H of Tyr103.

(a conserved residue that helps form the structure of the active site and may stabilize the transition state during catalysis).

Assignment of 3′-GMP Resonances. Two sets of resonances are observed for 3′-GMP when it is in molar excess of barnase; thus, the bound and free ligand are in slow exchange on the chemical shift time scale. This is not unexpected for a dissociation constant of 2.3 μM for the barnase–3′-GMP complex. The ^{1}H resonances of 3′-GMP bound to barnase were assigned as follows. The anomeric proton of ribose, H1′, has a characteristic chemical shift of 5.3–6.0 ppm (Wüthrich, 1986). Very few protein resonances are observed in this chemical shift range in the spectra of free barnase. Consequently, the H1′ resonance of barnase-bound 3′-GMP was easily assigned by identifying a set of new COSY, TOCSY, and NOESY cross peaks at 5.91 ppm in the spectra of the complex (Figure 5). COSY, TOCSY, and NOESY peaks are observed between H1′ and a resonance at 4.83 ppm which was assigned to H2′. A weak TOCSY and a NOESY peak are observed between H1′ and a resonance at 4.93 ppm, which has COSY, TOCSY and NOESY peaks with H2′. The resonance at 4.93 ppm was therefore assigned to H3′. Initially, H4′ could not be identified because no connectivities between H3′ and H4′ could be established. New COSY and TOCSY cross peaks are observed between resonances at 4.92 and 4.03 ppm. Also, NOEs are observed between H1′, H2′ and H3′, and the resonance at 4.03 ppm. On the basis of the similarity of the chemical shift of 4.03 ppm to the chemical shift of 3.98 ppm for H5′/H5″ in free 3′GMP, this resonance was tentatively assigned to H5′/H5″. The resonance at 4.92 ppm was assigned to H4′ in the complex, although the chemical shift of H4′ in free 3′-GMP is quite different, 4.51 ppm. With these assignments it is clear that no correlation can be observed between H3′ and H4′ because of the similarity in their chemical shifts. Originally, spectra of the complex were collected at 37 °C since all the studies on free barnase were carried out at this temperature and free barnase gels at temperatures above approximately 40 °C. In order to try to resolve the ambiguity in the assignments, spectra were obtained at higher temperatures. It was found that spectra of the complex could be acquired at temperatures up to 49 °C, although the sample is only stable for a few hours at this temperature. At progressively higher temperatures, the NOE between H1′ and H3′ resolves into two NOEs, as does the NOE between H5′H5″ and H3′. This is supporting evidence for the assignments of H3′ and H4′.

The H8 resonance of the guanine ring has no scalar couplings to any other protons in the ligand, and so it cannot be assigned using COSY and TOCSY spectra. It is, however, close in space to various protons of the ribose ring (Wüthrich, 1986) and so can be identified using NOEs. A set of new NOEs was identified in the spectra of the complex between a sharp resonance at 8.23 ppm and H1′, H2′, H3′, and H5′/H5″ (Figure 5). This resonance was assigned to H8. The chemical shift of 8.23 ppm is similar to that of 8.06 for H8 in free 3′-GMP. The network of intramolecular NOEs between H8, H1′, H2′, and H3′, and the resonances at 4.92 and 4.03 ppm, is further evidence that these resonances correspond to H4′ and H5′/H5″. Most of the resonances of 3′-GMP exhibit significant, moderate changes in chemical shift in the 3′-GMP–barnase complex relative to free 3′-GMP: H1′, –0.13 ppm; H2′, –0.09 ppm; H3′, 0.05 ppm; H4′, 0.41 ppm; H5′/H5″, 0.05 ppm; H8, 0.12 ppm.

Angle Restraints for Barnase. All the angle restraints derived from NOE and coupling constant data for free barnase were also obtained for barnase complexed with 3′-GMP. Additional χ_1 restraints were obtained for Ser57 ($-90° < \chi_1 < -30°$) and Asp101 ($30° < \chi_1 < 90°$) in the complex due to new assignments for Ser57 and better resolution of the resonances of Asp101.

Investigation of Possible Angle Restraints for 3′-GMP in the Complex. The conformation of nucleotides can be specified in terms of the pseudorotation phase angle, *P*, which describes the conformation of the sugar ring, and the glycosidic torsion angle, χ, which describes the orientation of the base relative to the sugar (Altona & Sundaralingam, 1972). The glycosidic torsion angle and sugar pucker are often restrained during the calculation of the structures of DNA duplexes and RNA. Accordingly, the possibility of using similar restraints for 3′-GMP in the complex was investigated.

The vicinal coupling constant between H1′ and H2′, $J_{1'2'}$, can be used to obtain information about the conformation of the ribose ring. $J_{1'2'}$ varies from 1–2 Hz for a C3′-endo conformation to 8 Hz for C2′-endo (Altona & Sundaralingam, 1973; de Leeuw & Altona, 1982). The value of $J_{1'2'}$ for 3′-GMP bound to barnase was measured using the method of Ludvigsen et al. (1991). This method was originally derived for measuring NH–C$^\alpha$H coupling constants in proteins, but the principles of the method also apply to measuring $J_{1'2'}$. $J_{1'2'}$ was found to be approximately 7.0 ± 1 Hz. This value is intermediate between the values for C2′-endo and C3′-endo and could indicate that the sugar has a conformation that is intermediate between C2′-endo and C3′-endo or that the ribose samples different conformations. Consequently, the sugar pucker was not restrained in the structure calculations. Using a two-state model that allows for only C2′-endo and C3′-endo states, the percentage of the C2′-endo conformer in solution

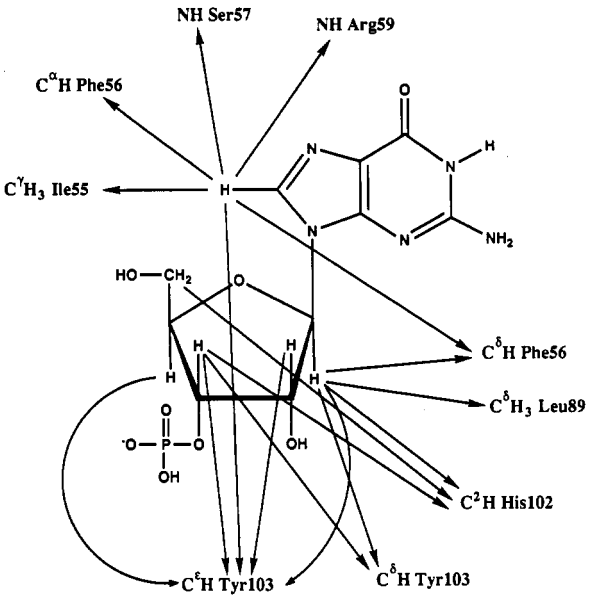

FIGURE 6: Intermolecular NOEs in the barnase–3′-GMP complex. The NOEs are represented by arrows.

can be roughly estimated as $10J_{1'2'}$ (Altona & Sundaralingam, 1973). According to this model, the conformation of the ribose ring of 3′-GMP in the complex is a mixture of approximately 72% C2′-endo and 28% C3′-endo conformers.

Free 3′-GMP has much narrower line widths than 3′-GMP bound to barnase. This allows $J_{1'2'}$ for free 3′-GMP to be measured directly from the splitting in the H1′ resonance in a 1D ^{1}H spectrum. The splitting is 5.6 Hz at 37 °C, pH 4.5. This corresponds to a mixture of 56% C2′-endo and 44% C3′-endo. Thus, there seems to be a small shift in the conformational equilibrium toward C2′-endo for 3′-GMP bound to barnase relative to free 3′-GMP.

The NOEs between H8 of the guanine ring and sugar protons can be used to obtain information about the glycosidic torsion angle (Wüthrich, 1986). There is no value of χ that is exactly consistent with the intensity of the observed NOEs for 3′-GMP bound to barnase. This indicates that conformational isomerization is probably occurring about the glycosidic bond. Consequently, the glycosidic torsion angle was not restrained. Instead, the observed intramolecular NOEs for 3′-GMP were converted into nine distance restraints, and these were used in the structure calculations.

Intramolecular NOEs of Barnase. The NOEs for barnase in the barnase–3′-GMP complex were analyzed in detail and compared with those of free barnase. A total of 966 intramolecular NOE distance restraints were obtained for barnase in the complex, compared with 887 for free barnase. More NOEs are resolved in the spectra of the complex due to the improved dispersion of resonances of nuclei in the active site, particularly in the guanine binding loop and the loop containing His102 (residues 99–105). Some NOEs cannot be compared because, owing to chemical shift changes, different NOEs are resolved in the spectra of the two species. However, almost all of the NOEs for free barnase are not affected by 3′-GMP binding. There are a few new NOEs and some small changes in the intensity of NOEs for some protons in the active site. Most of these are for resonances that exhibit large changes in chemical shift in the guanine binding loop and His102 loop.

Intermolecular NOEs. Intermolecular NOEs were identified between 3′-GMP and various active site residues. These are shown diagrammatically in Figure 6. These NOEs were converted into 17 intermolecular distance constraints.

Table I: Hydrogen/Deuterium Exchange Rates for NH Groups in Free Barnase and Barnase Complexed with 3′-GMP[a]

NH group[b]	exchange rate (min^{-1}) free barnase	exchange rate (min^{-1}) barnase-3′-GMP	ratio[c]
I4, mc	1.2×10^{-2}	1.9×10^{-2}	0.6
N5, sc	8.9×10^{-3}	3.2×10^{-2}	0.3
T6, mc	2.9×10^{-3}	4.0×10^{-3}	0.7
T16, mc	1.5×10^{-5}	2.5×10^{-5}	0.6
H18, mc	7.2×10^{-6}	1.9×10^{-5}	0.4
L20, mc	8.8×10^{-4}	9.5×10^{-4}	0.9
N23, mc	1.7×10^{-2}	2.2×10^{-2}	0.8
N23, sc	3.8×10^{-3}	1.4×10^{-2}	0.3
Y24, mc	6.8×10^{-3}	6.0×10^{-3}	1.1
T26, mc	1.3×10^{-5}	3.1×10^{-5}	0.4
K27, mc	7.1×10^{-4}	4.9×10^{-4}	1.4
E29, mc	9.3×10^{-3}	7.8×10^{-3}	1.2
A32, mc	2.2×10^{-4}	1.9×10^{-4}	1.2
G34, mc	1.4×10^{-3}	1.5×10^{-3}	0.9
W35, sc	1.5×10^{-2}	9.2×10^{-3}	1.6
V36, mc	4.5×10^{-5}	2.9×10^{-5}	1.6
K39, mc	4.4×10^{-3}	2.2×10^{-2}	2.0
N41, mc	1.7×10^{-2}	6.7×10^{-3}	1.5
N41, sc	2.0×10^{-3}	5.0×10^{-3}	0.4
A43, mc	8.9×10^{-4}	9.9×10^{-4}	0.9
E44, mc	2.5×10^{-4}	3.0×10^{-4}	0.8
V45, mc	6.7×10^{-6}	2.0×10^{-5}	0.4
I55, mc	3.0×10^{-3}	2.2×10^{-3}	1.4
N58, mc	$>1 \times 10^{-1}$	2.5×10^{-2}	>4
N58, sc	9.7×10^{-3}	7.7×10^{-3}	1.3
R59, mc	$>1 \times 10^{-1}$	4.4×10^{-2}	>2
G61, mc	$>1 \times 10^{-1}$	1.2×10^{-3}	>80
K62, mc	3.3×10^{-2}	1.1×10^{-3}	30
L63, mc	2.6×10^{-4}	6.3×10^{-6}	41
W71, sc	1.5×10^{-3}	1.1×10^{-5}	140
R83, sc	1.2×10^{-2}	4.6×10^{-3}	2.6
N84, sc	7.8×10^{-3}	3.0×10^{-2}	0.3
S92, mc	1.6×10^{-3}	4.7×10^{-3}	0.3
D93, mc	2.1×10^{-2}	2.1×10^{-2}	1.0
W94, mc	2.0×10^{-5}	1.7×10^{-5}	1.2
L96, mc	8.8×10^{-4}	7.1×10^{-4}	1.2
T100, mc	2.8×10^{-2}	6.2×10^{-2}	0.5
D101, mc	3.1×10^{-3}	2.4×10^{-4}	13
H102, mc	6.0×10^{-2}	2.5×10^{-3}	24
Y103, mc	2.7×10^{-3}	2.1×10^{-4}	13
Q104, mc	1.0×10^{-3}	1.4×10^{-5}	71
T105, mc	2.6×10^{-3}	1.6×10^{-4}	16
F106, mc	1.3×10^{-2}	1.0×10^{-2}	1.3
R110, mc	1.2×10^{-2}	4.5×10^{-2}	0.3

[a] Exchange rates were measured at 26 °C, pH 4.5. [b] mc and sc stand for main chain and side chain NH group, respectively. [c] The ratio is calculated by dividing the rate of exchange for barnase complexed with 3′-GMP by the rate for free barnase. The rates for main chain NH groups of residues 1–3, 5, 7–9, 28, 37, 38, 40, 42, 48, 54, 60, 65–68, 69–71, 78–83, 108, and 109 are too fast to be measured ($>1 \times 10^{-1}$ min^{-1}), and those of residues 10–15, 17, 19, 25, 30, 31, 33, 35, 36, 46, 49–53, 56, 72–76, 85, 87–91, 95, 97–99, and 107 are too slow ($<1 \times 10^{-5}$ min^{-1}). The main chain NH groups residues 22, 77, 84, and 86 could not be analyzed due to spectral overlap for either free wild-type barnase or the complex. The exchange rate of the main chain NH of residue 57 could not be analyzed in the complex because, although the cross peak is visible at 37 °C, it is not observable at 26 °C.

Hydrogen/Deuterium Exchange Rates. The exchange rate of NH hydrogens for deuterons was measured by following the decay with time of ^{15}N–^{1}H cross peaks in HSQC spectra of free barnase and the barnase–3′-GMP complex in D_2O. Using this method, exchange rates between approximately 1×10^{-1} and 1×10^{-5} min^{-1} were measured. These are summarized in Table I. Most protons have similar exchange rates in free and complexed barnase; however, the exchange of some protons in the active site is retarded by a factor of ~10–100 when 3′-GMP is bound. These include the main chain NHs of Asn58, Arg59, Gly61, Lys62, and Leu63 of the guanine binding loop, the side chain N$^{\epsilon}$H of Trp71 which

Table II: Structural Statistics

	barnase	barnase–3′-GMP		
	all[a]	all[a]	group A[b]	group B[c]
RMS deviation from average structure (Å)				
main chain[d]	0.69 ± 0.13	0.68 ± 0.12	0.63 ± 0.12	0.71 ± 0.20
all atoms[e]	1.37 ± 0.14	1.33 ± 0.14	1.23 ± 0.10	1.32 ± 0.18
RMS deviation of 3′-GMP conformation				
glycosidic torsion angle (χ) (deg)		141 ± 31	150 ± 2	99 ± 18
sugar pseudorotation angle (P) (deg)		226 ± 73	182 ± 4	334 ± 20
amplitude of ribose pucker (θ_m) (Å)		0.57 ± 0.08	0.60 ± 0.03	0.46 ± 0.08
RMS deviations from exp. distance restraints (Å)[f]				
all				
barnase–3′-GMP		0.048 ± 0.003	0.047 ± 0.002	0.047 ± 0.003
barnase	0.041 ± 0.003	0.044 ± 0.002	0.044 ± 0.002	0.043 ± 0.003
3′-GMP		0.119 ± 0.012	0.112 ± 0.009	0.125 ± 0.007
NOEs				
barnase–3′-GMP		0.045 ± 0.002	0.045 ± 0.002	0.045 ± 0.003
barnase	0.039 ± 0.003	0.041 ± 0.002	0.041 ± 0.002	0.040 ± 0.003
3′-GMP[d]		0.122 ± 0.012	0.115 ± 0.009	0.131 ± 0.007
hydrogen bonds				
barnase–3′-GMP		0.086 ± 0.012	0.086 ± 0.011	0.080 ± 0.009
barnase	0.071 ± 0.011	0.084 ± 0.012	0.084 ± 0.013	0.081 ± 0.009
3′-GMP		0.096 ± 0.027	0.092 ± 0.013	0.067 ± 0.011
RMS deviations from idealized covalent geometry				
bonds (Å)				
barnase–3′-GMP		0.0095 ± 0.0005	0.0093 ± 0.0005	0.0100 ± 0.0000
barnase	0.008 ± 0.0004	0.0090 ± 0.0002	0.0090 ± 0.0000	0.0088 ± 0.0004
3′-GMP		0.026 ± 0.005	0.024 ± 0.001	0.032 ± 0.002
angles (deg)				
barnase–3′-GMP		2.41 ± 0.05	2.38 ± 0.01	2.49 ± 0.01
barnase	2.23 ± 0.06	2.25 ± 0.07	2.25 ± 0.07	2.25 ± 0.01
3′-GMP		6.4 ± 0.9	5.8 ± 0.1	7.7 ± 0.1
impropers (deg)				
barnase–3′-GMP		1.10 ± 0.04	1.11 ± 0.04	1.06 ± 0.04
barnase	0.99 ± 0.03	1.06 ± 0.03	1.06 ± 0.03	1.04 ± 0.03
3′-GMP		1.93 ± 0.54	2.08 ± 0.50	1.57 ± 0.46
potential energies (kcal mol^{-1})[g]				
E_{VDW}				
barnase–3′-GMP		−246 ± 13	−248 ± 12	−240 ± 16
barnase	−242 ± 12	−271 ± 10	−271 ± 10	−266 ± 10
3′-GMP		26 ± 6	23 ± 6	27 ± 6
E_{NOE}				
barnase–3′-GMP		118 ± 13	117 ± 11	116 ± 17
barnase	69 ± 10	97 ± 11	98 ± 11	92 ± 15
3′-GMP		22 ± 4	19 ± 3	24 ± 2
E_{CDHI}	4.7 ± 1.3	7.0 ± 1.6	6.9 ± 1.7	6.9 ± 1.8

[a] Statistics for all 20 structures. [b] Statistics for the 12 group A structures of the complex and [c]*for* the five group B structures. Values are given as the root mean square ± 1 standard deviation. [d] Values are calculated for C^α, C, and N for residues 4–110. Residues 1–3 were excluded since they exhibit only sequential NOEs (Bycroft et al., 1991). The values for the 20 structures are relative to the average of the 20 structures. Similarly, the values for the 12 and five structures are relative to the corresponding averages. [e] Values are calculated for all atoms of residues 4–110 for free barnase and also the atoms of 3′-GMP for the complex. [f] For free barnase, 887 NOE distance restraints and 38 hydrogen-bond restraints, with each hydrogen bond being characterized by two distance restraints, r_{NH-O} = 1.8–2.0 Å and r_{N-O} = 2.7–3.0 Å, were used, and for the complex, 992 NOE distance restraints (966 intramolecular protein NOEs, nine intramolecular 3′-GMP NOEs, and 17 intermolecular NOEs) plus 42 hydrogen-bond restraints (38 intramolecular protein restraints and four intermolecular restraints) were used. [g] The force constants of the NOE, van der Waals repulsion and torsion angle terms were 50 kcal mol^{-1} Å^{-2}, 4 kcal mol^{-1} Å^{-4}, and 200 kcal mol^{-1} rad^{-2}, respectively.

packs onto the guanine binding loop, and the main chain NHs of Asp101, His102, Tyr103, Gln104, and Thr105. The maximum possible decrease in exchange rate for a K_d of 2.3 μM and 3′-GMP and protein concentrations of 5 mM is approximately 50-fold (Paterson et al., 1990). This is similar to the protection observed here for some protons ($N^\epsilon H$ of Trp71 and main chain NH of Gln104), which suggests that the exchange of these protons is greatly retarded in the complex. Other protons clearly can exchange in both the free and complexed state since they are only mildly protected.

Hydrogen-Bond Restraints. Amide exchange data and NOEs indicate that the same intramolecular protein hydrogen bonds are present in the barnase–3′-GMP complex and in free barnase (Bycroft et al., 1991). Accordingly, the same restraints for intramolecular protein hydrogen bonds were used for calculating the structure of the complex as for free barnase.

There is strong NMR evidence that the main chain amide protons of Arg59 and Ser57 make new hydrogen bonds in the barnase–3′-GMP complex. Both the main chain ^{15}N and NH resonances of Arg59 and Ser57 shift markedly downfield when 3′-GMP binds. Large downfield shifts of ^1H and ^{15}N resonances have been associated with the formation of hydrogen bonds in model systems and peptides (Live & Cowburn, 1987, and references therein). The changes in chemical shift in complexed barnase, particularly for the proton resonances, are too large to be caused by ring-current effects of the guanine ring (Giessner-Prettre & Pullman, 1976). In

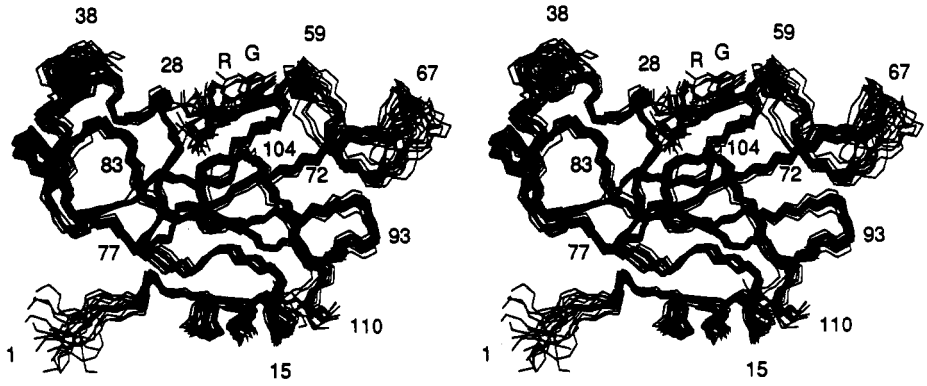

FIGURE 7: Superposition of the 20 calculated structures of the barnase–3′-GMP complex. The C, N, and C^{α} atoms of the protein main chain and 3′-GMP are shown. Some residues are labeled by number. The guanine ring and ribose of 3′-GMP are labeled "G" and "R", respectively.

addition, amide protons involved in hydrogen bonds are known to be protected against exchange with solvent. Although the exchange rate of the main chain NH of Ser57 could not be measured because this resonance is very weak in HSQC spectra at 26 °C, the exchange rate of Arg59 is decreased when 3′-GMP binds (Table I).

Since there is no major conformational change in barnase upon 3′-GMP binding, the hydrogen-bond acceptors for the NH groups of Ser57 and Arg59 must be located on the ligand. On the basis of the observed intermolecular NOEs, the only suitable groups on 3′-GMP are O6 and N7 of the guanine ring. Preliminary structure calculations revealed that the NH of Ser57 is hydrogen bonded to N7 and the NH of Arg59 is hydrogen bonded to O6. These hydrogen-bond constraints were then used in the subsequent calculations.

Structure Calculations of the Barnase–3′-GMP Complex. When all the distance and angle restraints for the protein and 3′-GMP were used in the first stage of the structure calculation, the chirality of the sugar carbons was often inverted, usually at C1′ or sometimes at C2′ or C3′. This may have been a consequence of the dihedral angle restraints being turned off during this stage of the calculation and/or the NOEs for 3′-GMP not being consistent with a single conformation. The second stage of the calculation could not change the chirality of sugar carbons. The problem of inversion of chirality was solved by using all the intramolecular protein restraints and only the intermolecular distance restraints for H8 of 3′-GMP in the first stage of the calculation and all the restraints for the protein and 3′-GMP in the second stage.

Using this procedure, a total of 20 structures of the barnase–3′-GMP complex were calculated; 87% (20 out of 23) of the first-stage structure calculations were completed successfully. The glycosidic torsion angle and sugar pucker of 3′-GMP were random after this first stage and the chirality of the nucleotide was correct. In the second stage of the calculation, 62% (20 out of 32) structures were refined successfully, according to the criterion of no violations of NOE restraints greater than 0.4 Å in the final structure. If a refinement was not successful, the first-stage structure was refined again using a different random number seed for the initial velocities. Up to three attempts were needed to refine some of the first stage structures. There is no correlation between the energy of a final structures and the number of refinements required to obtain the structure. The structural statistics for the final structures are summarized in Table II. The protein backbone and the 3′-GMP of the 20 calculated structures are shown in Figure 7. Figures 8 and 9 show views of 3′-GMP and side chains in the active site.

Overall, the calculated structures of the complex are in good agreement with the experimental data. None of the structures have violations of distance restraints greater than 0.4 Å. The nonbonded contacts are good, as evidenced by the negative value of the average van der Waals energy term, and the deviations from ideal geometry are small (Table II). On the whole, the structure of the protein is well defined in the complex. The RMS deviations between the structure of the protein in the complex and the average structure are quite low: 0.68 Å for main chain atoms and 1.33 Å for all atoms. These deviations are slightly lower than those for free barnase, which are 0.69 and 1.37 Å for main chain and all atoms, respectively. The differences are due to the conformations of residues in the guanine binding loop, Ser57-Asn58-Arg59-Glu60-Gly61, and other active site residues, particularly the side chains of Arg87, Asp101, and His102, becoming better defined in the complex. The improved definition of these residues is probably caused by both small changes in NOEs and increased steric limitations imposed by the 3′-GMP.

The 3′-GMP is located in the active site in all the structures, but its conformation varies. The conformations can be classified into two main groups: group A, consisting of 12 structures with a ribose pucker that is near C2′-endo ($P \sim 182 \pm 4°$) and a glycosidic torsion angle intermediate between syn and anti ($\chi \sim 150 \pm 2°$), and group B, consisting of five structures with a C2′-exo ribose pucker ($P \sim 334 \pm 20°$) and a glycosidic torsion angle near syn ($\chi \sim 99 \pm 18°$) (see Figures 8 and 9). The deviations from distance restraints and idealized geometry are consistently higher for 3′-GMP than for the protein for both groups of structures (Table II). In addition, the RMS deviation from the distance restraints and idealized geometry for the protein are slightly higher in the complex than in the free protein (Table II). There is little difference between the structural statistics for the protein for the two groups of structures. The deviations from distance restraints and idealized geometry for the protein are very similar for both groups. Also, the overall energy of the protein is similar, although the van der Waals energy is slightly lower for group A than group B, while the NOE energy is slightly higher for group A than group B. There are, however, systematic differences between the two groups in the structural statistics for 3′-GMP. The deviations from the NOE distance restraints, bond lengths, and angles are higher for group B, while the deviations from the hydrogen-bonding distance restraints and improper angles are higher for group A. The van der Waals and NOE energies for 3′-GMP are slightly lower for group A than group B.

The increased violations in the complex suggest that conformational isomerization is occurring and that it is impossible to calculate a single structure that satisfies all the restraints because these reflect a mixture of conformations. Consequently, the final structures are probably some sort of

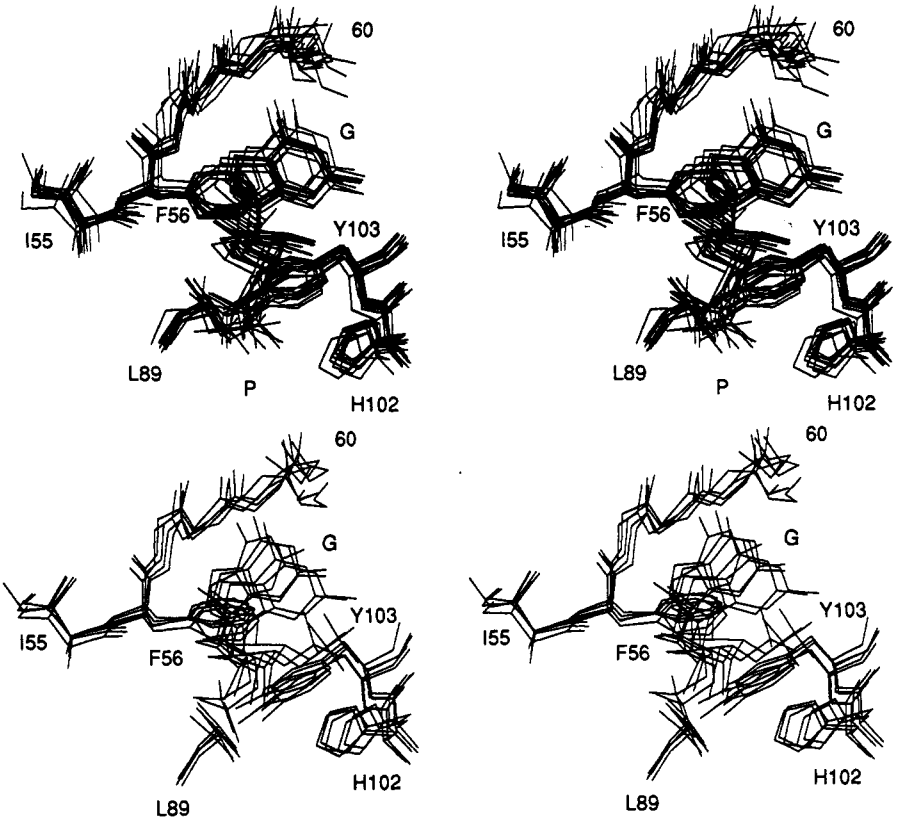

FIGURE 8: View of 3′-GMP and residues that have NOEs to 3′-GMP for (a, top) group A and (b, bottom) group B structures of the barnase–3′-GMP complex. Active site residues are labeled with single-letter amino acid code and residue number. The guanine ring of the 3′-GMP is labeled "G"and the phosphate is labeled "P".

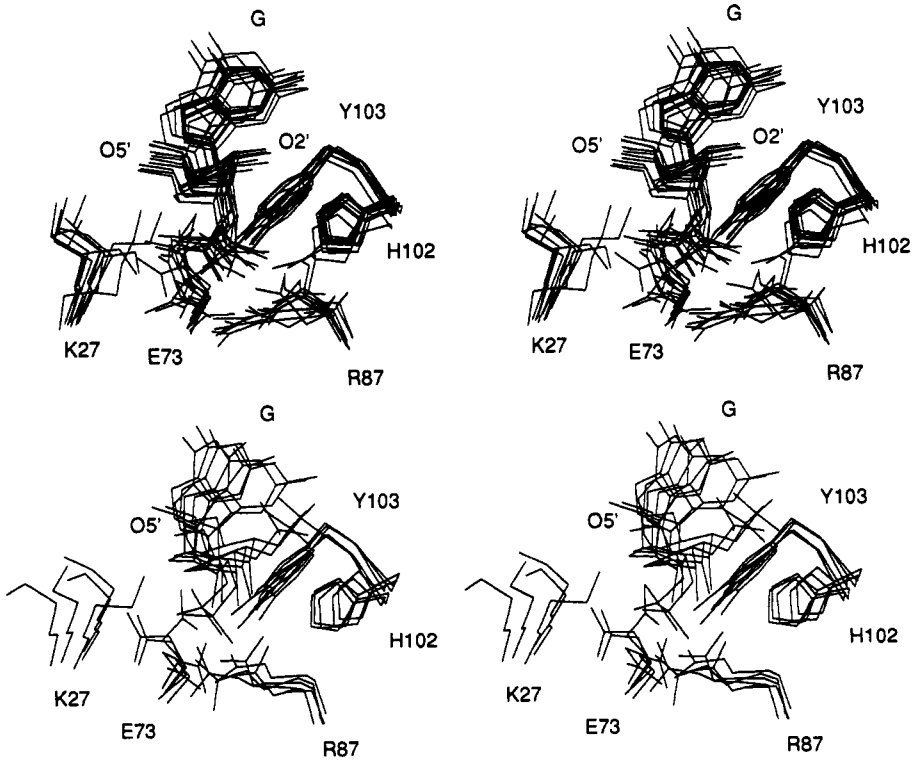

FIGURE 9: View of 3′-GMP and residues important for activity for (a, top) group A and (b, bottom) group B structures of the barnase–3′-GMP complex. Active site residues are labeled with single-letter amino acid code and residue number. The guanine ring, "G", and the O5′ of the 3′-GMP are also labeled.

time-averaged representation of the conformations sampled in solution. In order to check whether the 3′-GMP conformations in the calculated structures are reasonable or distorted by the requirements of satisfying NOEs for a mixture of conformations, the final structures were minimized using the program ENCAD (Levitt, 1983a,b; Dr. Miriam Hirshberg, personal communication). This program minimizes the conformation of 3′-GMP within the field of the protein which is held fixed during the calculation. Minimization caused very little change in the nucleotide conformations: θ_m

decreased slightly in the group A structures but did not change in the group B structures, while P and χ did not change significantly in either group. This suggests that the calculated 3′-GMP conformations are acceptable. It should be pointed out, however, that there is some controversy in the literature regarding the energetics of nucleotide conformations. Some theoretical studies predict that the ribose ring is extremely flexible and that the differences in energy between different ribose conformations are very small (Levitt & Warshel, 1978; Olson, 1982; Olson & Sussman, 1982), while others predict that the C2′-endo and C3′-endo conformations are much lower energy than other conformers (Murray-Rust & Motherwell, 1978; de Leeuw et al., 1980). Further support for the reasonableness of the calculated structures, however, is that their conformations are similar to those observed in different crystal structures of microbial ribonucleases complexed with nucleotides (Heinemann & Saenger, 1982; Arni et al., 1988; Koepke et al., 1989; Lenz et al., 1991b).

Although there are insufficient data to define the mixture of conformers for the complex, the equilibria for 3′-GMP bound to barnase and free in solution can be compared using simple models. A model of a two-state equilibrium between syn and anti conformers that does not account for sugar pucker can be used to calculate the percentage of syn conformer present in solution using NOE data and the following equation (Tran-Dinh et al., 1972):

$$\%(\text{syn}) = \frac{3\text{NOE}_{(\text{H8–H1}')}}{3\text{NOE}_{(\text{H8–H1}')} + \text{NOE}_{(\text{H8–H2}')} + \text{NOE}_{(\text{H8–H3}')}}$$

where $\text{NOE}_{(\text{H8–H1}')}$ is the intensity of the NOE between H8 and H1′, $\text{NOE}_{(\text{H8–H2}')}$ is the intensity of the NOE between H8 and H2′, and $\text{NOE}_{(\text{H8-H3}')}$ is the intensity of the NOE between H8 and H3′. The NOE intensities for barnase-bound 3′-GMP were obtained using volume integration by UXNMR of peaks in a NOESY spectrum with a 50-ms mixing time, at 37 °C, pH 4.5. From higher temperature spectra it is clear that there is no NOE between H8 and H4′, and so the NOE between H8 and H3′ can be measured accurately. Using the above equation, the conformation of 3′-GMP bound to barnase is calculated to be 69% syn. This is very similar to the values of 72–78% syn for free 3′-GMP at pH 8.9 and 1.4, respectively, reported by Tran-Dinh et al. (1972).

DISCUSSION

Interactions between Barnase and 3′-GMP. The studies reported here have identified several interactions that contribute to binding of 3′-GMP by barnase. Positively charged residues are involved in binding the phosphate group. The side chains of Lys27, Arg83, Arg87, and His102 in the calculated structures of the barnase–3′-GMP complex are near the phoshate group of 3′-GMP and could make electrostatic interactions with it (Figure 9). These results are similar to the crystallographic studies of binase complexed with 3′-GMP, where all four side chains make hydrogen bonds with phosphate (Drs A. G. Pavlovsky and M. Ya. Karpeisky, personal communication). Site-directed mutagenesis and NMR studies have shown that Lys27, Arg87, and His102 are important for binding of phosphate by barnase (Meiering et al., 1991). The guanine base interacts with residues in the conserved guanine binding loop in barnase (Figure 8). The main chain NH of Ser57 and Arg59 make hydrogen bonds with the N7 and O6 of the guanine ring, respectively, based on chemical shift changes, intermolecular NOEs, and changes in hydrogen/deuterium exchange rates. The aromatic rings of Phe56 and Tyr103 have NOEs with the H8 of the guanine ring and pack onto it. Overall, the binding of the guanine base by barnase is structurally similar to the binding observed in the crystal structures of complexes of various microbial ribonucleases with nucleotides (Sevcik et al., 1990).

Effects of 3′-GMP Binding on Protein Structure. On the basis of the NMR data, 3′-GMP binding causes very little change in the structure of barnase. The NOEs and coupling constants for free and complexed barnase are very similar, and consequently the calculated structures are very similar. Some conformational changes that have not been detected may occur for side chains in the active site whose conformations are not well defined by the NMR data. Some small conformational changes may also occur for the main chain of the guanine binding loop, where small changes in NOEs occur. The minimal conformational change in barnase upon 3′-GMP binding is similar to the results obtained in X-ray crystallography and NMR studies of nucleotide binding to other microbial ribonucleases (Heinemann & Hahn, 1989; Sevcik et al., 1990; Shimada & Inagaki, 1990). There is, however, a significant difference between the results obtained here and those obtained for RNase T1 by X-ray crystallography. The conformation of the peptide bond between the conserved asparagine of the guanine binding loop (Asn58 in barnase) and the preceding residue changes when nucleotides bind to RNase T1: the main chain ϕ angle for the asparagine is positive when nucleotides are bound and negative when the guanine binding site is empty (Martinez-Oyanedel et al., 1991). This contrasts with the results on barnase where the ϕ angle for Asn58 is positive in both the barnase–3′-GMP complex and free barnase studied by NMR and crystallography (Baudet & Janin, 1991; Mauguen et al., 1982). It is possible that the results for RNase T1 may be caused by crystal contacts in the vicinity of the guanine binding loop.

Effects of 3′-GMP Binding on Protein Dynamics. In contrast to the lack of structural change in barnase upon 3′-GMP binding, the NMR data indicate that significant dynamic changes do occur. The rotation of the ring of Phe56 becomes hindered when 3′-GMP binds. This probably results from a direct steric hindrance of ring rotation resulting from the packing of the guanine onto this side chain.

The effect of 3′-GMP binding on barnase dynamics is also reflected in the hydrogen/deuterium exchange rates of NH groups. The exchange rates of several NH groups within the active site of barnase are decreased upon 3′-GMP binding while those in the rest of the protein are unaffected. In protein–ligand complexes, NH groups may become protected against exchange *via* several mechanisms. The ligand may form a hydrogen bond to the protected proton, or there may be a decrease in structural fluctuations in the binding site, or the ligand may decrease the accessibility of exchangeable protons to solvent (Englander & Kallenbach, 1984). As discussed above, for the amide protons of Ser57 and Arg59 there is strong evidence for the formation of intermolecular hydrogen bonds when 3′-GMP binds. Nine of the ten other protected protons form hydrogen bonds with other residues in barnase. The hydrogen bond partners are NH Gly61–CO Asn58, NH Lys62–O^{δ} Asn5, NH Leu63–O^{δ} Asn58, $N^{\epsilon}H$ Trp71–CO Pro64, NH Asp101–O^{γ} Thr99, NH His102–CO Ser85, NH Tyr103–O^{γ} Thr99, NH Gln104–O^{δ} Asp101, NH Thr105–O^{δ} Asp101. These hydrogen bonds are in two active site loops and between one of these loops and part of the β-sheet. The increase in protection for these protons is probably the result of decreased structural fluctuations in these regions upon 3′-GMP binding. The amide proton of Asn58 is not hydrogen bonded in either free barnase or in the complex. The decrease

in the exchange rate for this residue is, therefore, probably the result of a reduction in solvent accessibility.

Preliminary measurements of $^{1}H-^{15}N$ NOEs, which are sensitive to dynamic processes on the microsecond to picosecond time scale (London, 1980; Kay et al., 1989), reveal that the mobility of the $N^{\epsilon}H$ group of Arg59 is decreased when 3′-GMP binds. Thus, 3′-GMP binding seems to cause the active site to become less mobile but has little effect on the dynamics of the rest of the protein.

The results on barnase are similar to those obtained for RNase T1. There is NMR evidence that the active site of RNase T1 also becomes more rigid when nucleotides bind (Shimada & Inagaki, 1990). The rotation of several aromatic residues in the active site becomes hindered or slow in complexes of RNase T1 with nucleotides. This is found for the equivalent residue to Phe56 of barnase and some other residues that are not found in barnase. Molecular dynamics simulations, time-resolved fluorescence measurements, and crystallographic temperature factors also indicate that the active site of RNase T1 becomes more rigid when nucleotides bind (MacKerell et al., 1989).

Conformations of 3′-GMP Bound to Barnase. The present studies reveal that 3′-GMP samples different conformational states when it is bound to barnase. This is evident from both coupling constant and NOE data and from the high residual violations for 3′-GMP in the calculated structures. The structure calculation protocol used here tries to simultaneously satisfy all the input restraints, and so the final structures are some sort of time average of the conformational equilibria in solution. It would be interesting to carry out molecular dynamics simulations to investigate further conformational isomerization.

Conformational isomerization may also occur for 3′-GMP bound to other microbial ribonucleases. Different conformations are observed for 3′-GMP bound to different enzymes, and for some complexes the electron density for the sugar is low or not apparent (Sugio et al., 1985; Pavlovsky et al., 1987; Sevcik et al., 1991; Lenz et al., 1991a). This suggests that various conformations may be sampled by nucleotides bound to these enzymes and that the particular conformer that is observed in the crystal state depends on the particular crystallographic conditions. In addition, NMR studies on RNase T1 suggest that crystal packing affects the conformation of bound nucleotides. Inagaki et al. (1985) found that the sugar conformation for 2′-GMP and 3′-GMP was C3′-endo, on the basis of measurements of $J_{1'2'}$. This is different from the C2′-endo conformation observed in crystal structures. Although Inagaki et al. concluded that the conformation of the nucleotides bound to RNase T1 was syn, on the basis of the observation of a strong NOE between H8 and H1′, no other intramolecular nucleotide NOEs were measured, and so conformational isomerization would not have been detected. Thus, it seems likely that conformational isomerization may be occurring for 3′-phosphate nucleotides bound to other microbial ribonucleases.

Relation of Structural Studies to Activity. In the proposed catalytic mechanism for the microbial ribonucleases, Glu73 interacts with the O2′-H of the guanine nucleotide, while His102 interacts with the O5′ of the nucleotide leaving group. The oxygens attached to the phosphorus of 3′-GMP (excluding the O3′ of the phosphoester bond) can be considered to be analagous to the O5′ of the substrate. In both the group A and group B structures of the barnase–3′-GMP complex, His102 is fairly close to the phosphate (Figure 9). In the group A structures the O2′-H is rotated away from the catalytic residues. In the group B structures, however, Glu73 is near the O2′-H and could hydrogen bond to it. Thus, the conformation of 3′-GMP is probably closer to that required for catalysis in the group B structures than in the group A structures. Allowing for small conformational changes for the nucleotide and active site residues, a catalytically productive situation could clearly be achieved.

As 3′-GMP is the product of hydrolysis, however, one would not expect it to be bound in a catalytically productive conformation all of the time. Rather, one would expect the enzyme to minimize its interactions with the product in order to promote dissociation. Consistent with this, the conformational isomerization observed for 3′-GMP bound to barnase is similar to that for free 3′-GMP. The present studies and those on other enzymes suggest that the microbial ribonucleases may, in general, make as weak interactions as possible with the product in order to promote dissociation.

ACKNOWLEDGMENT

We thank Dr. Miriam Hirshberg (MRC Unit for Protein Engineering, Cambridge) for carrying out the energy minimization calculations and Andrea Hounslow for assistance with the NMR experiments.

REFERENCES

Altona, C., & Sundaralingam, M. (1972) *J. Am. Chem. Soc. 94*, 8205–8212.

Altona, C., & Sundaralingam, M. (1973) *J. Am. Chem. Soc. 95*, 2333–2344.

Arni, R., Heinemann, U., Tokuoka, R., & Saenger, W. (1988) *J. Biol. Chem. 263*, 15358–15368.

Baudet, S., & Janin, J. (1991) *J. Mol. Biol. 219*, 123–132.

Bax, A., Mitsuhiko, I., Kay, L. E., Torchia, D. A., & Tschudin, R. (1990) *J. Magn. Reson. 86*, 304–318.

Bodenhausen, G., & Ruben, D. L. (1980) *Chem. Phys. Lett. 69*, 185–188.

Brooks, B. R., Bruccoleri, R. E., Olafson, B. D., States, D. J., Swaminthan, S., & Karplus, M. (1983) *J. Comput. Chem. 4*, 187–217.

Brünger, A. T. (1988) XPLOR Manual, Yale University, New Haven, CT.

Bycroft, M., Sheppard, R. N., Lau, F. T.-K., & Fersht, A. R. (1990) *Biochemistry 29*, 7425–7432.

Bycroft, M., Ludvigsen, S., Fersht, A. R., & Poulsen, F. M. (1991) *Biochemistry 30*, 8697–8701.

Dawson, R. M. C., Elliot, D. C., Eliot, W. H. E., & Jones, K. M. (1986) *Data for Biochemical Research*, Clarendon Press, Oxford.

Day, A. G., Parsonage, D., Ebel, S., Brown, T., & Fersht, A. R. (1992) *Biochemistry 31*, 6390–6395.

de Leeuw, F. A. A. M., & Altona, C. (1982) *J. Chem. Soc., Perkin Trans. 2*, 375–384.

de Leeuw, H. P. M., Haasnoot, C. A. G., & Altona, C. (1980) *Isr. J. Chem. 20*, 108–126.

Englander, S. W., & Kallenbach, N. (1984) *Q. Rev. Biophys. 16*, 521–655.

Giessner-Prettre, C., & Pullman, B. (1976) *Biopolymers 15*, 2277–2286.

Gronenborn, A. M., Bax, A., Wingfield, P. T., & Clore, G. M. (1989) *FEBS Lett. 243*, 93–98.

Hartley, R. W. (1980) *J. Mol. Evol. 15*, 355–358.

Hartley, R. W. (1988) *J. Mol. Biol. 202*, 913–915.

Hartley, R. W. (1989) *Trends Biochem. Sci. 14*, 450–454.

Heinemann, U., & Saenger, W. (1982) *Nature (London) 299*, 27–31.

Heinemann, U., & Hahn, U. (1989) in *Protein-Nucleic Acid Interaction* (Saenger, W., & Heinemann, U., Eds.) pp 111–142, MacMillan Press, London.

Hill, C., Dodson, G., Heinemann, U., Saenger, W., Mitsui, U., Nakamura, K., Borisov, S., Tischenko, G., Polyakov, K., & Pavlovsky, S. (1983) *Trends Biochem. Sci. 8*, 364–369.
Inagaki, F., Shimada, I., & Miyazawa, T. (1985) *Biochemistry 24*, 1013–1020.
Jones, D. N. M., Bycroft, M., Lubienski, M. J., & Fersht A. R. (1993) *FEBS Lett.* (in press).
Kay, L. E., Torchia, D. A., & Bax, A. (1989) *Biochemistry 28*, 8972–8979.
Koepke, J., Maslowska, M., Heinemann, U., & Saenger, U. (1989) *J. Mol. Biol. 206*, 475–488.
Lenz, A., Heinemann, U., Maslowska, M., & Saenger, W. (1991a) *Acta Crystallogr. B 47*, 521–527.
Lenz, A., Cordes, F., Heinemann, U., & Saenger, W. (1991b) *J. Biol. Chem. 266*, 7661–7667.
Levitt, M. (1983a) *J. Mol. Biol. 168*, 595–620.
Levitt, M. (1983b) *J. Mol. Biol. 168*, 621–657.
Levitt, M., & Warshel, A. (1978) *J. Am. Chem. Soc. 100*, 2607–2613.
Live, D. H., & Cowburn, D. (1987) *Biochemistry 26*, 6415–6422.
Loewenthal, R., Sancho, J., & Fersht, A. R. (1991) *Biochemistry 30*, 6775–6779.
London, R. E. (1980) *Magn. Reson. Biol. 1*, 1–69.
Ludvigsen, S., Andersen, K. V., & Poulsen, F. M. (1991) *J. Mol. Biol. 217*, 731–736.
MacKerell, A. D., Jr., Nilsson, L., Rigler, R., Heinemann, U., & Saenger, W. (1989) *Proteins: Struct., Funct., Genet. 6*, 20–31.
Marion, D., & Wüthrich, K. (1983) *Biochem. Biophys. Res. Commun. 113*, 967–974.
Marion, D., Driscoll, P. C., Kay, L. E., Wingfield, P. T., Bax, A., Gronenborn, A. M., & Clore, G. M. (1989) *Biochemistry 28*, 6150–6156.
Martinez-Oyanedel, J., Choe, H.-W., Heinemann, U., & Saenger, W. (1991) *J. Mol. Biol. 222*, 335–352.
Mauguen, Y., Hartley, R. W., Dodson, E. J., Dodson, G. G., Bricogne, G., Chothia, C., & Jack, A. (1982) *Nature (London) 297*, 162–164.
Meiering, E. M., Bycroft, M., & Fersht, A. R. (1991) *Biochemistry 30*, 11348–11356.
Morris, G. A., & Freeman, R. (1979) *J. Am. Chem. Soc. 101*, 760–762.
Mossakowska, D. E., Nyberg, K., & Fersht, A. R. (1989) *Biochemistry 28*, 3843–3850.
Murray-Rust, P., & Motherwell, S. (1978) *Acta Crystallogr. B 34*, 2534–2546.
Olson, W. K. (1982) *J. Am. Chem. Soc. 104*, 278–286.
Olson, W. K., & Sussman, J. L. (1982) *J. Am. Chem. Soc. 104*, 270–278.
Osterman, H. L., & Walz, F. G., Jr. (1978) *Biochemistry 17*, 4124–4130.
Osterman, H. L., & Walz, F. G., Jr. (1979) *Biochemistry 18*, 1984–1988.
Pace, C. N., Heinemann, U., Hahn, U., & Saenger, W. (1991) *Angew. Chem. 30*, 343–360.
Paterson, Y., Englander, S. W., & Roder, H. (1990) *Science 249*, 755–759.
Pavlovsky, A. G., Strokopytov, B. V., Borisova, S. N., Vainstein, B. K., Karpeisky, M. Y., & Iakovlev, G. I. (1987) *Dokl. Akad. Nauk SSSR 292*, 1253–1256.
Saenger, W. (1991) *Curr. Opin. Struct. Biol. 1*, 130–138.
Sevcik, J., Sanishvili, R. G., Pavlovsky, A. G., & Polyakov, K. M. (1990) *Trends Biochem. Sci. 15*, 158–162.
Sevcik, J., Dodson, E. J., & Dodson, G. G. (1991) *Acta Crystallogr. B 47*, 240–253.
Shaka, A. J., Barker, P. B., & Freeman, R. (1985) *J. Magn. Reson. 64*, 547–553.
Shaka, A. J., Lee, C. J., & Pines, A. (1988) *J. Magn. Reson. 77*, 274–293.
Shimada, I., & Inagaki, F. (1990) *Biochemistry 29*, 757–764.
Steyaert, J., Hallenga, K., Wyns, L., & Stanssens, P. (1990) *Biochemistry 29*, 9064–9072.
Sugio, S., Oka, K.-I., Ohishi, H., Tomita, K., & Saenger, W. (1985) *FEBS Lett. 183*, 115–118.
Takahashi, K., & Moore, S. (1982) *The Enzymes 15*, 435–467.
Tran-Dinh, S., Guschlbauer, W., & Guéron, M. (1972) *J. Am. Chem. Soc. 94*, 7903–7911.
Uchida, T., & Egami, F. (1971) *The Enzymes 4*, 205–250.
Walz, F. G., Jr., & Hooverman, L. L. (1973) *Biochemistry 24*, 4846–4851.
Wüthrich, K. (1986) *NMR of Proteins and Nucleic Acids*, Wiley, New York.